

Antiferromagnetic magnons in diluted triangular and *kagomé* lattices

D. L. Huber

Department of Physics, University of Wisconsin-Madison, Madison, Wisconsin 53706

W. Y. Ching

Department of Physics, University of Missouri-Kansas City, Kansas City, Missouri 64110

(Received 3 August 1992; revised manuscript received 12 October 1992)

Numerical results are presented for the local field distribution and the distribution of linearized magnon modes in diluted triangular and *kagomé* lattices. A nearest-neighbor antiferromagnetic Heisenberg spin Hamiltonian is assumed, and the linearization is carried out with respect to classical ground states obtained by means of an energy-minimization algorithm. In the case of the triangular lattice, the density of states associated with a 20% vacancy concentration is used to calculate the magnon contribution to the specific heat. With an exchange integral inferred from the Curie-Weiss constant, quantitative agreement is obtained with the experimental results for $\text{La}_{0.2}\text{Gd}_{0.8}\text{CuO}_2$ reported by Ramirez *et al.* over the interval $0.1 \text{ K} \leq T \leq 0.2 \text{ K}$. The behavior of the diluted *kagomé* lattice is compared with that of the triangular array. In contrast to the latter, the local fields in the diluted *kagomé* lattice take on the discrete values $2JS$, JS , and 0 . In the case of a 14% vacancy concentration, the distribution of magnon modes resembles that of the fully occupied array with a noncoplanar ground state. The relevance of these results to the behavior of $\text{SrCr}_8\text{Ga}_4\text{O}_{19}$ is discussed.

I. INTRODUCTION

Understanding the interplay of quantum fluctuations and thermal fluctuations that occurs in two-dimensional Heisenberg antiferromagnets with geometrical frustration is proving to be a challenging problem. In the case of systems with triangular coordination symmetry, the analysis is further complicated by the fact that in two of the compounds that have been extensively studied, GdCuO_2 (triangular) and $\text{SrCr}_8\text{Ga}_4\text{O}_{19}$ (*kagomé*), the magnetic lattices are diluted,¹ making direct comparison between experiment and theory difficult.

The purpose of this paper is to present the results of numerical studies of the local fields and magnetic excitations in diluted triangular and *kagomé* lattices with nearest-neighbor antiferromagnetic Heisenberg interactions. The calculations were done within the framework of a linear magnon approximation based on an expansion about a classical noncollinear ground state obtained by using an energy-minimization or quench algorithm² which entails successively rotating each spin into the direction of its local field until the total energy stabilizes. In the case of the triangular lattice, detailed calculations of the distribution of local fields, the magnon density of states, and the magnon contribution to the specific heat are carried out for a 20% vacancy concentration. The results for the specific heat are compared with the experimental data for $\text{La}_{0.2}\text{Gd}_{0.8}\text{CuO}_2$ reported by Ramirez, Jager-Waldau, and Siegrist.³ Calculations of the distribution of local fields and the magnon density of states were carried out for the *kagomé* lattice with 14% vacancies. Here the comparison is made with the theoretical results for the fully occupied lattice.^{4,5} For reasons which will be discussed below, it was not possible to make meaning-

ful contact with experiment.

The results for the triangular lattice are presented in Sec. II and those for the *kagomé* lattice in Sec. III. Section IV is devoted to a brief summary and discussion. Since the numerical methods that were used are discussed in Ref. 2, they will not be treated in any detail in this paper.

II. TRIANGULAR LATTICE

The Hamiltonian used in the studies of the diluted triangular (and *kagomé*) lattice is of the standard isotropic Heisenberg form:

$$\mathcal{H} = J \sum' \mathbf{S}_j \cdot \mathbf{S}_k, \quad (1)$$

where \mathbf{S} is the spin, J is the exchange integral, and the prime signifies that the summation is limited to nearest-neighbor (j, k) pairs. As noted in the Introduction, the analysis of the diluted system involves a calculation of the magnon energies that is based on an approximation in which the equations of motion of the spin operators are linearized with respect to a ground-state (more precisely, equilibrium) spin configuration which is determined from an energy-minimization algorithm discussed in Ref. 2. The corresponding calculation for the fully occupied triangular lattice has been carried out by Jolicoeur and Le Guillou⁶ who obtained analytic expressions for the magnon energies. This was possible since the ground state of the fully occupied lattice has long-range order (in the spin-wave approximation).

A measure of the effect of dilution on the degree of spin order is provided by the distribution of local fields associated with the ground-state spin configurations. In the fully occupied lattice, the local fields are identical in

magnitude at each site, with the value $3JS$. In the case of the diluted lattice, the distributions of local fields were calculated from ground-state configurations determined from the energy-minimization algorithm.² The calculations were carried out for an array of 33×33 sites with periodic boundary conditions. The results shown in Fig. 1 are for a single configuration of 218 vacancies corresponding to 80% occupancy of the array, with the vacancies being distributed at random. From this figure, it is evident that the local fields range continuously from $\approx JS$ to $\approx 3.5JS$, indicating that short-range order is virtually destroyed by the dilution.

The vectors specifying the ground-state spin orientations are used to determine the elements of a dynamical matrix whose eigenvalues are the magnon energies.² The distribution of magnon modes obtained from five vacancy configurations in 33×33 arrays with 80% occupancy are shown as a histogram in Fig. 2(a). Particularly noteworthy is the quasilinear behavior below $E \approx 2.5JS$. For comparison, the distribution of magnon modes in a fully occupied 33×33 array is shown in Fig. 2(b). As expected, the distribution for the fully occupied array shows far more structure which will, of course, be smoothed out in the large- N limit, N being the number of spins.

As mentioned earlier, in the compound GdCuO_2 , the magnetic ions occupy sites on a triangular lattice.^{1,3} Since Gd^{3+} is an S -state ion, the magnetic properties should be well described by a Heisenberg Hamiltonian with $S = \frac{7}{2}$, apart from dipolar effects. So far, it has not been possible to prepare bulk samples with more than 80% Gd occupancy, with the remaining sites being occupied by the diamagnetic La^{3+} ions.³ Since the Gd spin is large, the linear magnon analysis discussed above is an appropriate starting point in making a comparison between experiment and theory.

Assuming the nearest-neighbor approximation is appropriate, a value for the exchange integral can be obtained from the Curie-Weiss temperature, -12.5 K, by means of the equation

$$T_{\text{CW}} = -\frac{1}{3} \langle z \rangle JS(S+1), \quad (2)$$

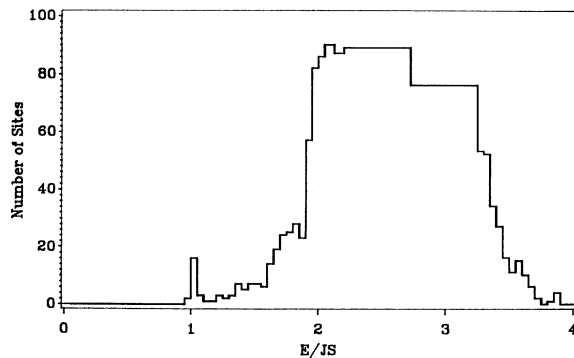


FIG. 1. Distribution of local fields in a 33×33 triangular array with 20% vacancies distributed at random. Periodic boundary conditions. One vacancy configuration. In the fully occupied array, all local fields are equal to $3JS$.

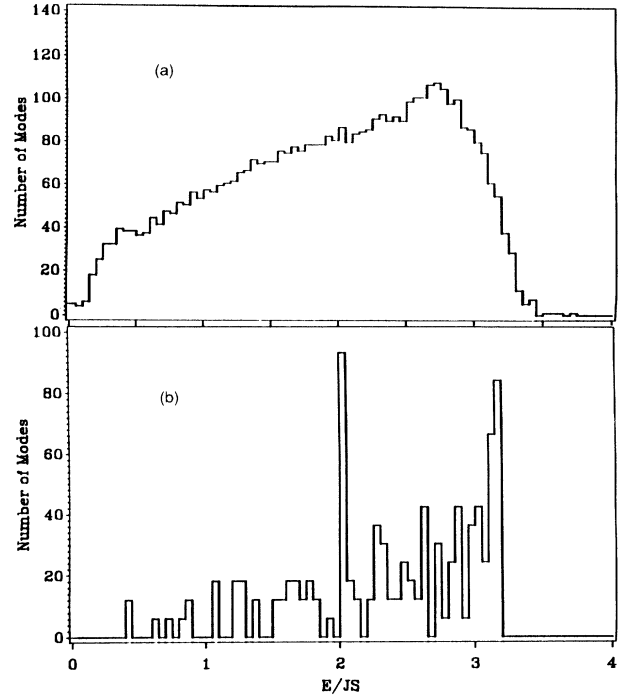


FIG. 2. (a) Distribution of magnon energies in a 33×33 array with 20% vacancies distributed at random. Periodic boundary conditions. Five vacancy configurations. (b) Distribution of magnon energies in a 33×33 triangular array with no vacancies. Periodic boundary conditions.

where $\langle z \rangle$ is the average number of nearest neighbors, $6 \times 0.8 = 4.8$, corresponding to 80% random occupancy. From this equation, one obtains the value $J = 0.50$ K for the exchange integral.

Having determined J , one can calculate the magnon contribution to the specific heat by means of the standard boson expression

$$C_{\text{mag}} = k \sum_{\nu} (E_{\nu}/kT)^2 \exp(E_{\nu}/kT) [\exp(E_{\nu}/kT) - 1]^{-2}, \quad (3)$$

where ν designates the magnon mode. Figure 3 shows a

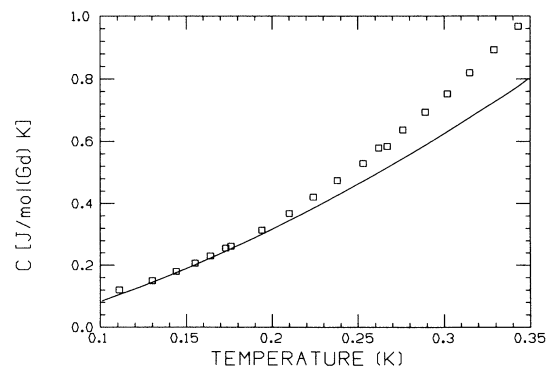


FIG. 3. Specific heat of $\text{La}_{0.2}\text{Gd}_{0.8}\text{CuO}_2$ vs T . Open squares: data from Ref. 3. Solid line: C_{mag} calculated from Eq. (3) with $J = 0.50$ K. Magnon energies from five configurations of a 33×33 array with 20% vacancies.

comparison between the calculated and measured values of the specific heat for $\text{La}_{0.2}\text{Gd}_{0.8}\text{CuO}_2$ over the interval $0.10 \leq T \leq 0.35$ K, the upper limit being one-half of T_g ; the spin-glass temperature, which is equal to 0.7 K.³ From this figure it is evident that there is quantitative agreement between experiment and theory for $0.1 \leq T \leq 0.2$ K. Above 0.25 K the theoretical curve begins to deviate appreciably from the data. Although this deviation might reflect the onset of a significant lattice contribution, the small value of the specific heat in the singlet ground-state system PrCuO_2 (Ref. 3) argues against this interpretation. A more likely cause is the failure of the linear magnon approximation as T approaches T_g .

In Ref. 1, the point is made that the specific heat of the quasi-two-dimensional Gd (triangular lattice) and Cr (*kagomé* lattice) compounds varies approximately as T^2 in the spin-glass phase, in contrast to the nearly linear behavior found in three-dimensional spin glasses such as $\text{Eu}_{0.4}\text{Sr}_{0.6}\text{S}$ and $\text{Cd}_{0.8}\text{Mn}_{0.2}\text{Te}$. Figure 4 displays a log-log plot of the calculated values of C_{mag}/T vs T , which shows quasilinear behavior for $0.1 \leq T \leq 0.2$ K. It should be noted that the numerical calculations of C_{mag} begin to produce unphysical results below 0.06 K, a result that is attributable to finite-size effects which prevent an accurate determination of the low-lying, spatially extended modes.

It is important to compare the values of C_{mag} in the diluted lattice with what would be obtained from a fully occupied array in the low-temperature limit. According to Ref. 6, the three magnon modes vary linearly with wave vector q in the long-wavelength limit:

$$E_1 = 9JSqa \quad (4a)$$

and

$$E_2 = E_3 = (9/2^{1/2})JSqa, \quad (4b)$$

where a is the distance between nearest neighbors. Using (3a) and (3b) and the previously determined value for J , one finds

$$C_{\text{mag}} [J/\text{mol}(\text{Gd}) \text{K}] = 0.17T^2, \quad (5)$$

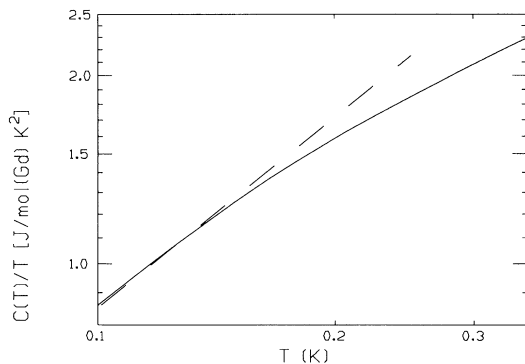


FIG. 4. log-log plot of $C_{\text{mag}}(T)/T$ vs T . The solid line is a replot of the theoretical curve in Fig. 4. The dashed line shows the region of quasilinear behavior.

which is approximately 50 times smaller than the measured value at 0.1 K.

III. *kagomé* LATTICE

The *kagomé* lattice can be obtained from the triangular lattice by removal of 25% of the sites. The effect of this decimation on the ground state and low-lying excitations is profound, even in the linear spin-wave approximation. As noted, the triangular lattice with nearest-neighbor antiferromagnetic exchange interactions has long-range order in the classical limit.⁶ In contrast, the classical ground state of the nearest-neighbor Heisenberg antiferromagnet on the fully occupied *kagomé* lattice is highly degenerate.^{4,5} Recent Monte Carlo studies have shown that the system exhibits local nematic (coplanar) spin order at low temperatures with a correlation length that diverges as $T \rightarrow 0$.⁵

The calculations of Ref. 5 were limited to the fully occupied *kagomé* lattice. In this section results are presented for the effect of a 14% vacancy concentration on the distribution of the local fields and the linearized spin excitations. In the fully occupied lattice, all local fields are equal to $2JS$. The distribution of local fields obtained with 14% of the spins removed is shown in Fig. 5, which displays the combined results from three vacancy configurations in an array of 675 sites with periodic boundary conditions. From this figure, it is evident that nearly all (>96%) have a local field equal to $2JS$, as in the fully occupied system, while the remainder have local fields equal to JS or 0. Thus, *unlike* the triangular lattice, the local field distribution remains discrete under dilution. Similar results were also obtained with 19 and 27% vacancy concentrations, the only difference being the relative change in the fraction of sites with local field equal to JS or 0. In the case of a 675-site array with 19% vacancy concentration, 514 spins had local field $2JS$, 33 had local field JS , and 2 had a local field equal to zero. With 27% vacancies, 416 spins had local field $2JS$, 75 had local field JS , and 4 had local field equal to zero (single configurations at each concentration).

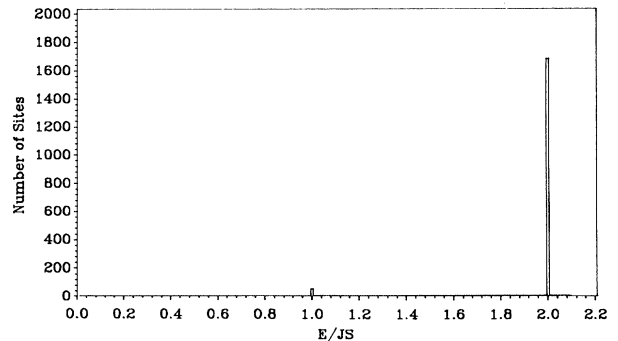


FIG. 5. Distribution of local fields in a 675-site *kagomé* array with 14% vacancies distributed at random. Periodic boundary conditions. Combined data from three vacancy configurations. In the fully occupied lattice, all sites have a local field equal to $2JS$. In the diluted arrays, a total of 1680 spins had local field $2JS$, 51 had local field JS , and 12 had a local field equal to 0.

Although it is clear from the analysis of Ref. 5 that any complete account of the dynamics of even the *classical* Heisenberg antiferromagnet on the *kagomé* lattice must include the nonlinear terms in the equations of motion for the spin operators, it is still of interest to ascertain the effects of dilution on the linearized magnon modes. Figure 6(a) shows the distribution of magnon modes in a representative fully occupied, noncoplanar ground-state configuration with 675 spins. It is evident that the distribution is continuous with a relatively sharp peak near $E=0$ and a broad peak near $E=1.5JS$. Figure 6(b) shows the resulting magnon distribution obtained by combing the data from three vacancy configurations of a 675-site array with 14% dilution. The distribution is seen to resemble that of the fully occupied noncoplanar array. It should be noted, however, that the peak near $E=0$ is enhanced by a total of 27 zero-frequency modes, whereas in the fully occupied noncoplanar array, there were only three such modes.

Efforts were made to calculate the distribution of magnon modes in fully occupied arrays with coplanar ground-state spin configurations. However, the dynamical matrix could not be numerically diagonalized due to the large number of zero-frequency modes.⁵ Some indication of the behavior that might be expected is provided by the calculations of Zeng and Elser⁴ who investigated the dynamics in a triangular lattice with a weak coupling to the spins that are eliminated in the decimation process leading to the *kagomé* net. According to Fig. 6 of Ref. 4,

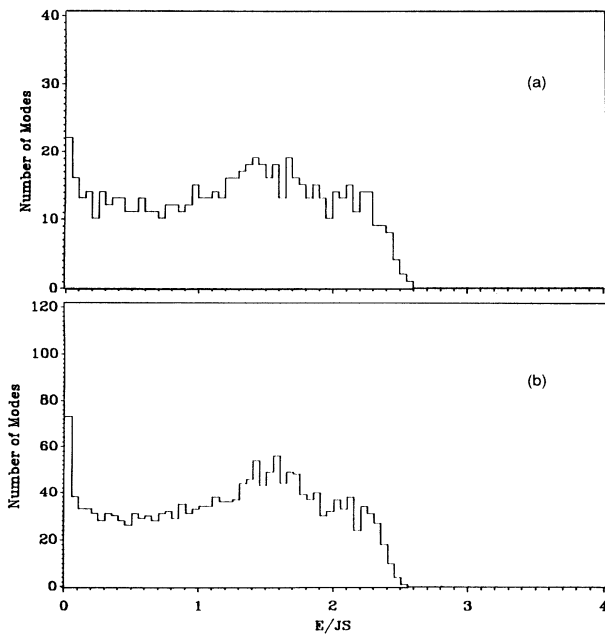


FIG. 6. (a) Distribution of magnon energies in a fully occupied 675-site *kagomé* array. Periodic boundary conditions. One configuration. Noncoplanar ground state. (b) Distribution of magnon energies in a 675-site *kagomé* array with 14% vacancies distributed at random. Periodic boundary conditions. Combined data from three vacancy configurations. Ground states are noncoplanar.

the density of states, aside from the zero-frequency modes, should show peaks near $0.4JS$ and $2JS$, with a continuum of modes filling in the gap between the peaks.

In the case of the diluted arrays, a limited study was carried out that showed for a given vacancy distribution, the coplanar equilibrium spin configurations (obtained by starting the energy minimization procedure with an array where the spins were coplanar, but randomly oriented in the plane) were higher in energy by several percent than the noncoplanar configurations obtained with no restriction on the relative spin orientations. This result suggests that dilution acts to weaken the tendency toward nematic order. Whether this happens abruptly or slowly is an open question.

In the Introduction, it was pointed out that the compound $\text{SrCr}_8\text{Ga}_4\text{O}_{19}$ was an example of a Heisenberg antiferromagnet on a *kagomé* lattice. To be more precise, the Cr ions in this compound occupy the $12k$, $12a$, and $4f$ sites of the $P6_3/mmc$ space group. The $12k$ sites form a *kagomé* lattice with 86% Cr occupation.⁷ Experimental studies of the specific heat and susceptibility indicate a spin-glass transition at $T \approx 3.5$ K. Below T_g , the magnetic contribution to the specific heat varies as T^2 , similar to $\text{La}_{0.2}\text{Gd}_{0.8}\text{CuO}_2$.⁸

Of particular relevance to this paper is the question of whether the spin-glass transition and the quadratic behavior of the specific heat are characteristic of the *nearest-neighbor* Heisenberg antiferromagnet on the diluted *kagomé* lattice. Although a definite answer to this question cannot be given at this time, the insensitivity of the local field distribution to dilution argues against this interpretation. Furthermore, on the basis of the analysis of Ref. 5, one would expect that lowest-energy magnon modes would be strongly influenced by anharmonic effects, in contrast to triangular lattice systems like $\text{La}_{0.2}\text{Gd}_{0.8}\text{CuO}_2$. As a consequence, the specific heat in the nearest-neighbor system is unlikely to vary as T^2 over an appreciable range of temperature. A more plausible explanation is that the spin-glass phase and the quadratic variation of the specific heat reflect the presence of longer-range interactions.

Alternatively, Chubukov has shown for the nearest-neighbor Heisenberg antiferromagnet on the fully occupied *kagomé* lattice that quantum fluctuations can lift the degeneracy of the ground state and restore long-range order.⁹ In addition, the spin-wave excitations have a finite stiffness which is a factor of $S^{-1/3}$ smaller than is the case of conventional spin waves. Whether the equivalent diluted system has a spin-glass transition and quadratic variation of the specific heat below T_g when quantum effects are taken into account remains to be answered.

IV. SUMMARY AND DISCUSSION

The purpose of this paper has been to analyze the effects of dilution on the local field distribution and the magnon density of states in two two-dimensional geometrically frustrated Heisenberg antiferromagnets. The magnon energies were calculated in the linear approximation starting from a classical ground state obtained using an energy-minimization algorithm. In the case of the tri-

angular lattice, diluting the system broadened the local field distribution and modified the density of states. Calculations of the magnon contribution to the specific heat with the density of states appropriate to a 20% vacancy concentration and a nearest-neighbor exchange integral inferred from the high-temperature susceptibility were in good agreement with the experimental results for $\text{La}_{0.2}\text{Gd}_{0.8}\text{CuO}_2$ over the interval $0.1 \leq T \leq 0.2$ K. The agreement between the measured and calculated values of the specific heat parallels similar agreement obtained previously for CuMn (Ref. 2), $\text{Eu}_x\text{Sr}_{1-x}\text{S}$,¹⁰⁻¹³ and $\text{Cd}_{1-x}\text{Mn}_x\text{Te}$.¹⁴ In these three-dimensional spin glasses, calculated values of the (linearized) magnon contribution to the specific heat, carried out using independently determined values of the exchange interactions, were in good agreement with experiment at low temperatures. The behavior of the other system studied, the Heisenberg antiferromagnet on the diluted *kagomé* lattice, is more difficult to understand. Instead of a continuous distribution of local fields, almost all spins have a local field equal to $2JS$, the value appropriate to the undiluted system. Similarly, the distribution of magnon modes in the presence of a 14% vacancy concentration resembles that of the undiluted lattice in a *noncoplanar* ground state.

The calculations discussed here pertain to zero temperature. In the case of the triangular lattice, it is expected that they are quantitatively accurate for large S when $kT \ll JS$, as appears to be the case for $\text{La}_{0.2}\text{Gd}_{0.8}\text{CuO}_2$ below 0.2 K. They are also expected to be qualitatively

correct for the spin- $\frac{1}{2}$ case (provided the system has the same long-range order as in the classical limit). At this point, it is not clear as to their applicability to the nearest-neighbor *kagomé* system even at $T=0$. Non-linear terms in the equations of motion are expected to be important, and the interplay between dilution and quantum fluctuations is likely to be important but subtle. Furthermore, the likely presence of longer-range interactions (as well as anisotropy), albeit weak, make the interpretation of the experimental results in $\text{SrCr}_8\text{Ga}_4\text{O}_{19}$ in terms of an isotropic Hamiltonian with nearest-neighbor interactions problematical.

Note added in proof. Recently E. F. Shender, V. B. Cherepanov, P. C. Holdsworth, and A. J. Berlinsky (unpublished) showed how the discrete distribution of local fields arises in the diluted *kagomé* system. In particular, they established that sites with local field equal to JS are associated with pairs of vacancies.

ACKNOWLEDGMENTS

The authors would like to thank Dr. A. P. Ramirez for providing them with a copy of the $\text{La}_{0.2}\text{Gd}_{0.8}\text{CuO}_2$ data presented in Ref. 3. D.L.H. would also like to thank E. F. Shender and V. B. Cherepanov for helpful comments and communicating results of their work, and A. Chubukov for providing a copy of his work on quantum fluctuations.

¹A. P. Ramirez, J. Appl. Phys. **70**, 5952 (1991).

²L. R. Walker and R. E. Walstedt, Phys. Rev. B **22**, 3816 (1980).

³A. P. Ramirez, R. Jager-Waldau, and T. Siegrit, Phys. Rev. B **43**, 10461 (1991).

⁴C. Zeng and V. Elser, Phys. Rev. B **42**, 8436 (1990).

⁵J. T. Chalker, P. C. W. Holdsworth, and E. F. Shender, Phys. Rev. Lett. **68**, 855 (1992).

⁶Th. Jolicoeur and J. C. Le Guillou, Phys. Rev. B **40**, 2727 (1989).

⁷A. Obradors, A. Labarta, A. Isalgué, J. Tejada, J. Rodriguez, and M. Pernet, Solid State Commun. **65**, 189 (1988).

⁸A. P. Ramirez, G. P. Espinoza, and A. S. Cooper, Phys. Rev.

Lett. **64**, 2070 (1990); Phys. Rev. B **45**, 2505 (1992).

⁹A. Chubukov, Phys. Rev. Lett. **69**, 832 (1992).

¹⁰W. Y. Ching, D. L. Huber, and K. M. Leung, Phys. Rev. B **21**, 3708 (1980).

¹¹U. Krey, Z. Phys. B **38**, 243 (1980); **42**, 231 (1982); J. Magn. Mater. **28**, 231 (1982); J. Phys. (Paris) Lett. **46**, L845 (1985).

¹²J. Wosnitzer, H. v. Lohneysen, W. Zinn, and U. Krey, Phys. Rev. B **33**, 3436 (1986).

¹³W. Y. Ching and D. L. Huber, Phys. Rev. B **34**, 1960 (1986).

¹⁴W. Y. Ching and D. L. Huber, Phys. Rev. B **30**, 179 (1984).